The official journal of
INTERNATIONAL FEDERATION OF PIGMENT CELL SOCIETIES · SOCIETY FOR MELANOMA RESEARCH
PIGMENT CELL & MELANOMA Research

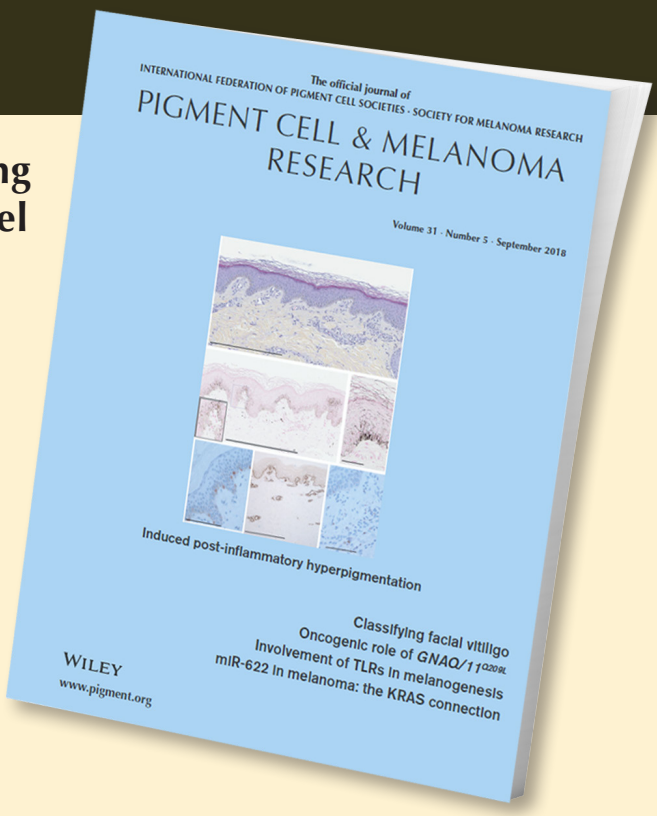

Refinement of the endogenous epitope tagging technology allows the identification of a novel NRAS binding partner in melanoma

Michal Alon | Rafi Emmanuel | Nouar Qutob | Anna Bakhman | Victoria Peshti | Alexandra Brodezki | David Bassan | Mickey Kosloff | Yardena Samuels

DOI: 10.1111/pcmr.12705
Volume 31, Issue 5, Pages 641–648

If you wish to order reprints of this article, please see the guidelines **here**

Supporting Information for this article is freely available **here**

EMAIL ALERTS
Receive free email alerts and stay up-to-date on what is published in Pigment Cell & Melanoma Research – **click here**

Submit your next paper to PCMR online at http://mc.manuscriptcentral.com/pcmr

Subscribe to PCMR and stay up-to-date with the only journal committed to publishing basic research in melanoma and pigment cell biology

As a member of the IFPCS or the SMR you automatically get online access to PCMR. Sign up as a member today at **www.ifpcs.org** or at **www.societymelanomaresarch.org**

To take out a personal subscription, please click here
More information about Pigment Cell & Melanoma Research at **www.pigment.org**

Received: 11 January 2018 | Accepted: 3 April 2018

DOI: 10.1111/pcmr.12705

SHORT COMMUNICATION

WILEY

Refinement of the endogenous epitope tagging technology allows the identification of a novel NRAS binding partner in melanoma

Michal Alon[1] | Rafi Emmanuel[1] | Nouar Qutob[1] | Anna Bakhman[2] | Victoria Peshti[1] | Alexandra Brodezki[1] | David Bassan[1] | Mickey Kosloff[2] | Yardena Samuels[1]

[1]Department of Molecular Cell Biology, Weizmann Institute of Science, Rehovot, Israel

[2]Department of Human Biology, Faculty of Natural Science, University of Haifa, Haifa, Israel

Correspondence
Yardena Samuels
Email: Yardena.samuels@weizmann.ac.il

Funding information
EU-H2020-ERC-POC, Grant/Award Number: 712730; ERC, Grant/Award Number: StG-335377; The Knell Family; Melanoma Research Alliance; The Hamburger Family; Israel Science Foundation, Grant/Award Number: 712811; Henry Chanoch Krenter Institute for Biomedical Imaging and Genomics; Estate of Alice Schwarz-Gardos; Estate of John Hunter; Peter and Patricia Gruber Award

Summary

The *NRAS* oncoprotein is highly mutated in melanoma. However, to date, no comprehensive proteomic study has been reported for NRAS. Here, we utilized the endogenous epitope tagging (EET) approach for the identification of novel NRAS binding partners. Using EET, an epitope tag is added to the endogenously expressed protein, via modification of its genomic coding sequence. Existing EET systems are not robust, suffer from high background, and are labor-intensive. To this end, we present a polyadenylation signal-trap construct for N'-tagging that generates a polycistronic mRNA with the gene of interest. This system requires the integration of the tagging cassette in frame with the target gene to be expressed. Using this design, we demonstrate, for the first time, endogenous tagging of *NRAS* in melanoma cells allowing the identification of the E3 ubiquitin ligase c-CBL as a novel NRAS binding partner. Thus, our developed EET technology allows the characterization of new RAS effectors, which could be beneficial for the design of future drugs that inhibit constitutive signaling of RAS oncogenic mutants.

KEYWORDS
endogenous epitope tagging, melanoma, NRAS

1 | INTRODUCTION

Cutaneous melanoma is mostly driven by somatic mutations. A recent comprehensive sequencing study of large cohorts has identified driver genes in melanoma and genomically classified the disease according to the most predominant mutated genes: mutant *BRAF*, mutant *NRAS*, mutant *NF1*, and Triple-WT (Network, 2015). *NRAS* is highly mutated in melanoma (15%–20%), yet, functional studies are needed to decipher the role of these mutations in melanomagenesis. Recently, the investigation of protein–protein interactions has become a focus of cancer research, mainly thanks to its ability to identify novel binding partners of mutant cancer proteins and study their function. RAS proteins have a dominant role in human cancer, and in particular NRAS in melanoma. The interactions between RAS oncoproteins and their effectors or regulators are unsolved at the proteomic level (Stephen, Esposito, Bagni, & Mccormick, 2014), possibly due to fast association and dissociation of most RAS/effector complexes (i.e., short-lived), which is compatible with the signaling function of these interactions in the cell (Erijman & Shifman, 2016). Therefore, we utilized the endogenous epitope tagging (EET) approach to search for NRAS interacting proteins in melanoma in an unbiased way. Endogenous epitope tagging is a powerful method to study the function of genes at their physiological levels. These include applications such as the purification of endogenous proteins and the identification of novel protein partners, validating novel

Michal Alon and Rafi Emmanuel contributed equally to this work.

protein–protein interactions discovered using other methodologies, or when specific antibodies are not available. In EET, the translational start or stop codon is replaced with a tagging epitope (e.g., Flag, HA, and c-myc) and a selection marker cassette, at the genomic level in a homologous recombination (HR)-mediated pathway. This substitution is directed by ~1 Kbs of homologous sequences flanking the ATG or the stop codon of the gene of interest on both sides. As HR is considered a rare event, only one of the alleles can be tagged. Using commercial antibodies, the tagged protein and the associated binding partners can be immunoprecipitated and subjected to proteomics analysis and characterization (Kim, Bonifant, Bunz, Lane, & Waldman, 2008). The constructs used for this application bear a recombinant adeno-associated virus (rAAV) backbone. rAAV vectors have been demonstrated to be efficient for gene targeting for the low integration into the genome and the induction of HR upon increasing the virus particles in the cells (Porteus, Cathomen, Weitzman, & Baltimore, 2003; Schnepp, Jensen, Chen, Johnson, & Clark, 2005). Following the cloning of the homology arms, the construct is encapsulated, and the cells are infected with the virus particles (Figure S1).

To apply EET on low infectable melanoma cells, we modified the plasmid previously published by Zhang et al., (Zhang et al., 2008), schematically described in Figure 1a. We constructed a polyadenylation signal-trap construct for N-terminus tagging (pT2A-Puro^r-User-N'). This construct generates a polycistronic mRNA of the tagged gene of interest and a selectable marker, separated by a self-cleaving 2A peptide that replaces the thymidine kinase promoter (pTK), which will be

Significance

Revealing RAS interacting proteins presents a promising strategy for drug design against defective RAS signaling in cancer in general and against oncogenic NRAS in melanoma in particular. This study demonstrates a new endogenous epitope tagging (EET) approach to tag the N' terminus of *NRAS* in melanoma cells without harming the functionality of the protein. This allowed the identification of a NRAS novel binding partner-c-CBL, which is an E3 ubiquitin-protein ligase that plays a role in melanoma cell proliferation, migration, and invasion. These findings suggest that implementation of the EET approach could allow us to unveil RAS effectors, as well as effectors of other driver genes in melanoma and other malignancies.

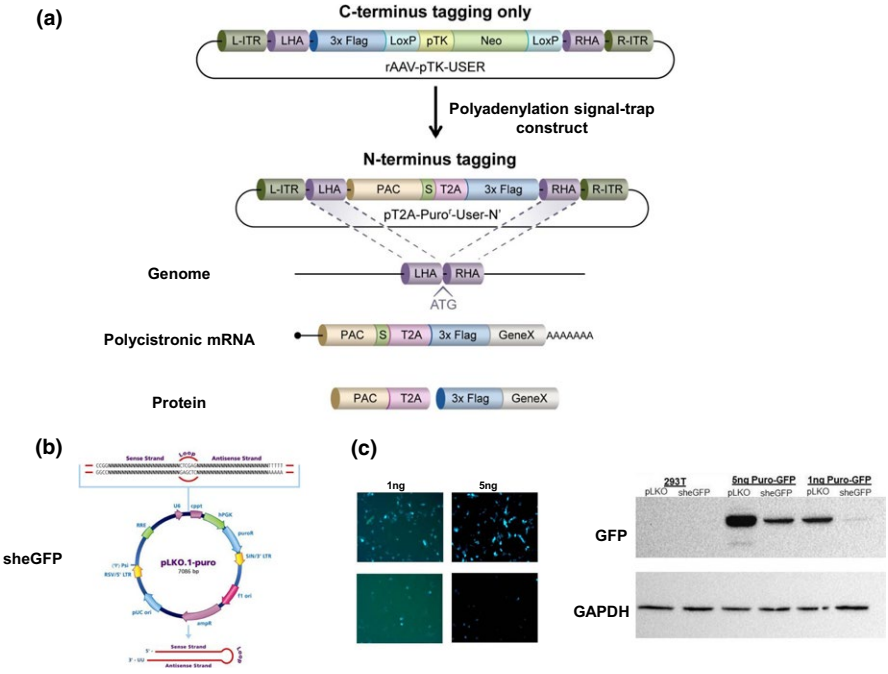

FIGURE 1 Development of efficient constructs for N-terminus endogenous epitope tagging (EET). (a) Schematic description of the developed EET construct. The construct was originated from the rAAV-pTK-USER (Schnepp et al., 2005). The rAAV-pTK-USER is suitable for C-terminus tagging following Cre-recombinase exclusion of selection marker. The developed construct does not have intrinsic promoter activity. The N-terminus plasmid is a polyadenylation signal-trap construct, which integrates the tagging cassette instead of the ATG of the gene of interest. This construct generates a polycistronic mRNA with the tagged allele, which is expressed without the need for Cre-recombinase exclusion of the selection marker. In the N-terminus tagging, the tag will contain only the last proline of the T2A peptide. Sequence from EGFP is cloned downstream to the selection marker and is recognized by a shRNA to selectively modulate the expression of the tagged allele. (b) Schematic description of the pLKO.1-neo vector used for the cloning of the sheGFP. (c) Representative images and blot demonstrating the knockdown efficiency of the sheGFP in 293T cells cotransfected with either 1 ng or 5 ng of plasmid expression EGFP and 1 μg of sheGFP. GAPDH was used to normalize the loading accuracy. (LHA, left homology arm; RHA, right homology arm; Neo, neomycin resistance gene; S, sheGFP) [Colour figure can be viewed at wileyonlinelibrary.com]

fused to the C-terminus of the selection marker. This design gives rise to a single reading frame, which requires the integration of the tagging cassette in frame with the target gene (Figure 1a). Furthermore, downstream to the selection marker we added a sequence that is recognized by sheGFP (Figure 1b,c), to enable us to specifically downregulate the expression of the tagged allele. To facilitates the cloning of the homologous arms into the EET constructs, we used the rapid one-step USER cloning technique for multiple fragments, as previously described (Bitinaite et al., 2007). In this construct design, the expression of the tagged allele does not necessitate exclusion of the selection marker cassette via Cre-recombinase, which would reduce the time required to obtain tag-containing cells. This design should also reduce the background of false-positive cells caused by the constitutively expressed selection markers.

Using the N-terminus tagging construct, we Flag-tagged the *NRAS* gene in different melanoma cells, which are either *wt* for *NRAS* or harbor the recurrent Q61R/K mutation. The cell genotypes, infection conditions, and the results of the tagging efficiency are summarized in Table S1. As described in Table S1, in most cases, multiple colonies were obtained in each well of 96-well plates and were screened as pools, using a forward primer located upstream to the LHA and a reverse primer located within the *PAC* gene of the tagging cassette (Figure 2a). A representative description of the genomic screen and validation at the mRNA are described in (Figure 2a,b). According to the results, the tagging efficiency was around 20%, even for polyploid cells like 12T (single clones) and for low-infected cells as 17T and 110T (~1% infection efficiency). We obtained following a screen of only one of 10 plates, 13 and 17 positive pools for 17T and 110T, respectively. Moreover, in the case of 12T cells (~15% infection efficiency), we obtained 10 positive single clones of 44 (22%). The highest tagging efficiency of ~40% was obtained from the highly infectable A375 cells (Table S1). Although we tagged cells that harbor the Q61 mutation, we obtained solely colonies that were tagged in their *wt* allele. Nevertheless, an extensive structural comparison of wt and Q61 mutants of different RAS isoforms showed they are essentially identical in structure (Figure S2). In particular, the region adjacent to the Q61 residue was similar in all of these structures, regardless of whether the position was a glutamine or a mutation to another residue, suggesting they bind partners similarly. Indeed, previous studies compared the binding affinity of wt versus mutant RAS to its various effectors and reached similar conclusions. Hunter et al. (2015) showed that wt and K-Ras-Q61 had similar

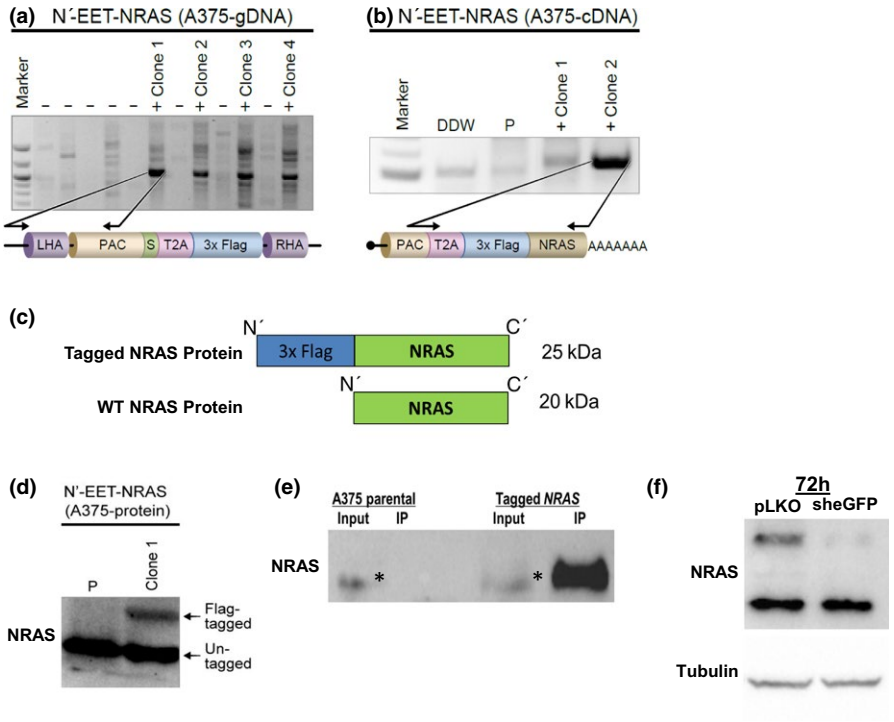

FIGURE 2 Validating the EET of *NRAS* in melanoma cell line. (a) Schematic description of the primers location used for the screen of the tagged allele at the genomic level and a representative agarose gel of the genomic DNA screen using primers that amplified the LHA of the N-terminus tagging of *NRAS* in A375 cells. (b) A schematic description of the tagged *NRAS* transcript and the location of the primers used for the validation of the expression of the tagged allele at the mRNA level. (P) indicates parental A375 cells, and (+) indicates positive *NRAS*-tagged cells. (c) Schematic description of N-terminus 3xFlag-tagged NRAS protein. (d) Western Blot analysis of lysates extracted from parental A375 cells (P) and A375 cells expressing the tagged *NRAS* allele, probed with anti-NRAS antibody. (e) A representative blot following immunoprecipitation (IP) using anti-Flag beads that were incubated with cell lysate of either parental A375 cells or a clone expressing the Flag-tagged *NRAS* allele. The membrane was then blotted with anti-NRAS antibody. Non-specific bands of the anti-NRAS antibody in the input are designated with an asterisk. (f) Representative blot demonstrating the knockdown efficiency of the tagged *NRAS* allele follow transfection with the sheGFP construct [Colour figure can be viewed at wileyonlinelibrary.com]

affinities for Raf. Chuang et al. (1994) measured similar affinities between wt and HRAS-Q61 mutants for c-Raf-1. In addition, Burd et al. (2014) observed similar interactions of wt and NRAS-Q61 mutants for RAF and PI3K. Therefore, all these previous studies showed that wt and Q61 RAS mutants bind effectors with similar affinity.

As the Flag-tag adds approximately 5 kDa to the size of the *wt* NRAS protein (Figure 2c), this enabled us to further validate the protein expression of the tagged allele by Western blot and immunoprecipitation in single clones of tagged A375 cells (Figure 2d, e). In addition, we demonstrated an efficient knockdown of the tagged allele at the protein level using sheGFP (Figure 2f).

An unexpected obstacle in the N-terminus tagging was a significant reduction in Flag-NRAS expression, compared to the *wt* allele (Figure 2d). We assumed that the sequence of the puromycin resistance gene (*PAC*), which is a foreign sequence rich in CpGs, may have induced silencing of the promoter of the tagged allele via methylation (Chevalier-Mariette et al., 2003; Mutskov & Felsenfeld, 2004). To test our assumption, we treated tagged and parental A375 cells with the general DNA methyltransferase inhibitor 5-azacitidine (5-aza). We found that the expression of the tagged allele significantly increased upon the addition of different concentrations of 5-aza, while the expression of the *wt* allele was hardly affected (Figure S3). Therefore, we consider replacing the *PAC* in future studies with a low-CpG *PAC* sequence or with a selective marker with less CpG in its sequence, such as a neomycin resistance gene.

Prior to performing functional studies on the endogenously tagged *NRAS*, we confirmed that the tagged NRAS is farnesylated and therefore active. RAS proteins undergo a lipid post-translational modification called farnesylation (Kho et al., 2004), which anchors NRAS to the membrane and is essential for its proper signaling activity (Nussinov, Tsai, Chakrabarti, & Jang, 2016). To this end, we examined the effect of adding the farnesyl transferase inhibitor lonafarnib to the two Flag-tagged NRAS clones A4 and F12 that were derived from the A375 melanoma cell line. We tested the mobility shifts of the Flag-NRAS in the presence of increasing concentrations of lonafarnib. Unprocessed (un-farnesylated) NRAS is known to migrate slower in SDS/PAGE than its farnesylated isoforms. The mobility-shift assay consisted of immunoprecipitation of the protein lysates with Flag beads, followed by SDS/PAGE and Western blotting, to determine whether the inhibition of farnesyl transferase changed the migration rate of the Flag-NRAS. After the addition of lonafarnib, only the slow un-farnesylated form of NRAS was detected, compared to the control where only the farnesylated, faster migrating band was detected (Figure 3a). These results indicate that the tagging of the NRAS protein did not affect its activity. We, therefore, next immunoprecipitated Flag-NRAS extracted from A375 single clones A4 using Flag beads with or without EGF activation followed by mass spectrometry (MS) analysis. One of the interactors that were identified by the MS analysis to significantly bind NRAS was c-CBL. Indeed, three CBL peptides were identified by MS analysis, both with and without EGF activation. The percentage of the protein sequence covered by identified peptides was 5.45%. The average area of the three unique peptides with the largest peak of the Flag-NRAS immunoprecipitated samples was 4.2e06 without EGF activation and 3.3e06 after EGF activation. These peptides were not identified in the isotype control. c-CBL an E3 ubiquitin-protein ligase, is responsible for the intracellular transport and degradation of a large number of tyrosine kinases; it is also known to function as a negative regulator of many signaling pathways that are triggered by activation of cell surface receptors (Schmidt & Dikic, 2005). Furthermore, STRING analysis showed a reported interaction between NRAS and CBL (Figure S4). Indeed, immunoprecipitation of Flag-NRAS from the A375 single clones A4 and F12 before and after EGF activation validated the interaction between NRAS and c-CBL. The immunoblots in Figure 3b show endogenous c-CBL after the pull down of the Flag-NRAS in both single clones, and the intensity of

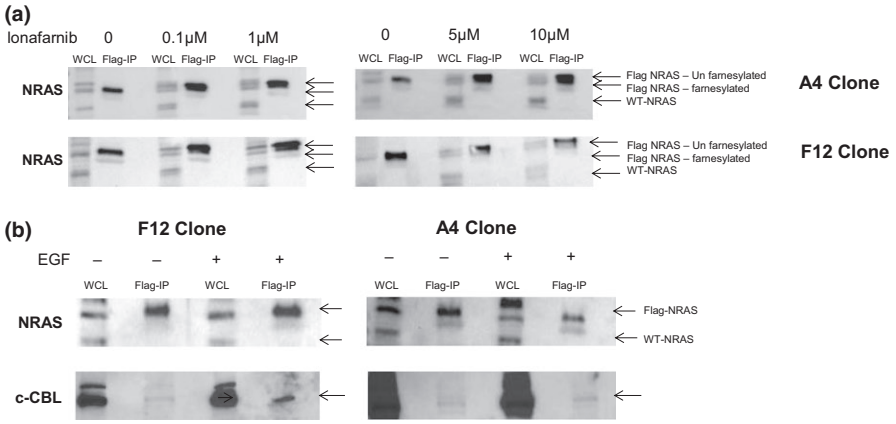

FIGURE 3 Functional analysis of Flag-NRAS. (a) Flag-NRAS A375 clones (A4 and F12) were incubated with increasing concentrations of lonafarnib (0.1,1, 5 and 10 μM) for 24 hr, followed by Flag immunoprecipitation and Western blotting with anti-NRAS to detect the farnesylated (faster migrating band) and un-farnesylated (slower migrating band) forms of Flag-NRAS.(b) Immunoblots of Flag-tagged NRAS A375 clones-A4 and F12-immunoprecipitated with anti-Flag before or after EGF activation. Immunoprecipitates were analyzed in parallel by anti-NRAS and anti-c-CBL immunoblotting. Flag-NRAS was co-immunoprecipitated with endogenous c-CBL from the two clones- A4 and F12 of Flag-tagged NRAS lysates using anti-c-CBL antibody. WCL – whole cells lysate

c-CBL is slightly increased after EGF induction in F12 clones. Thus, our results confirm that c-CBL is indeed a novel NRAS interacting protein. In addition, we transiently overexpressed wt NRAS or the NRAS-Q61R mutant protein in A375 melanoma cells; both wt and mutant NRAS were tagged with Flag at the N' terminus of NRAS protein. Flag-NRAS was immunoprecipitated by Flag beads. The immunoblots in Figure S5 show detection of the endogenous c-CBL after the pull down of the Flag-NRAS following overexpression of both wt NRAS and mutant NRAS. Therefore, the wt and the Q61R mutant Ras show similar binding to c-CBL.

CBL, which is highly expressed in human melanoma cells at the mRNA and protein levels, plays a role in melanoma cell proliferation, migration, and invasion. Knocking down of c-CBL by siRNA was followed by decreased proliferation, colony formation, migration, and invasion of melanoma cells (Nihal & Wood, 2016). Mutations in CBL and K-Ras or NRAS are mutually exclusive in JMML (Juvenile myelomonocytic leukemia) patients, indicating that CBL may play a role in deregulating the RAS pathway (Loh et al., 2009). Thus, the co-immunoprecipitation of c-CBL and NRAS supports a physiological relevant interaction between them, motivating future functional analyses on their roles in melanoma. Furthermore, the mass spectrometry data presented here reveal additional novel NRAS binding partners, the significance of which is currently being investigated.

In summary, our successful application of our novel design of the EET methodology allowed us to identify a novel interactor of one of the most important oncogenes in melanoma, NRAS (Network, 2015). Indeed, the constructs described here make EET a more efficient strategy, feasible even for cells with low infectability without harming the functionality of the tagged protein. In addition, the integration of an EGFP sequence targeted by a commercial shRNA enables us to modulate the expression of the tagged allele, thus expanding the repertoire of functional assays that can be performed without being restricted to antibody-related approaches such as IP, ChIP-seq, and immunohistochemistry. Thus, allowing us to better decipher the role of mutations in driver genes in different malignancies.

2 | MATERIAL AND METHODS

2.1 | Construction of pT2A-Puro^r-User-C'

The template for the preparation of the C-terminus tagging construct was rAAV-pTK-USER (5). The first step was cloning of the HA-tag instead of the 3xFlag-tag. The oligos SpeI_linker_HA_FW and EcoRI_linker_HA_Rev were annealed, filled-in with Klenow fragment, and cloned via SpeI and EcoRI. The pTK was replaced with T2A via EcoRI and MluI following the annealing and Klenow extension of the oligos EcoRI_T2A_FW and MluI+BglII_T2A_Rev. The last step was the cloning of the *PAC* gene without ATG and with the addition of sheGFP recognition sequence via BglII and EcoRV following PCR, using the primers BglII_PAC_FW and EcoRV+NdeI+T3 + sheGFP_PAC_Rev (the sequence of the primers is described in Table S2).

2.2 | Construction of pT2A-Puro^r-User-N'

The N-terminus tagging construct was prepared by a modulation of pT2A-Puro^r-User-C'. As a first step, a single nucleotide substitution was introduced in the LHA cloning site to eliminate an ATG codon, to interrupt the translation of the PAC. The construct was digested with AgeI and SpeI; the oligos AgeI_LHA cloning cassette_FW and SpeI_LHA cloning cassette_Rev were annealed and cloned. The PAC+sheGFP PCR product was amplified using the primers SpeI_PAC_FW and EcoRI_PAC+sheGFP_Rev and cloned via SpeI and EcoRI. The 3xFlag-tag was cloned via BglII and EcoRV following the annealing and extension of the oligos BglII_3xFlag_FW and EcoRV_3xFlag__Rev (Table S2).

2.3 | Cloning of the HAs into the tagging constructs

The constructs were digested with XbaI and Nt.BbvCI to obtain two fragments, large and small. The amplification of the HAs was performed using the KAPA HiFi HotStart Uracil ReadyMix (KapaBiosystems), according to the manufacturer protocol. The following sequences were added to the primers: for C-terminus tagging, LHA primers GGGAAAG(dU), and GGAGACA(dU)NB (N: A, T, C, and G; B: T, C, and G), for forward and reverse primers, respectively. RHA primers GGTCCCA(dU) and GGCATAG(dU) for forward and reverse primers, respectively. For N-terminus tagging, LHA primers GGGAAAG(dU) and GGAGACG(dU) for forward and reverse primers, respectively. RHA primers GGTCCCA(dU)NB and GGCATAG(dU), for forward and reverse primers, respectively. The products were desalted and assembled with the digested plasmid at a molar ratio of 1:10:10:10 (Large: Small: LHA:RHA) in a total of 9 μl to which 1 μl of USER™ Enzyme (Biolabs) according to the manufacturer instructions. The reaction was transformed into chemical competent cells by heat-shock. Positive colonies were validated by enzymatic digestion and sequencing (the sequences of the primers are described in Table S2).

2.4 | Virus preparation

7×10^6 low passage AAV-293 cells were seeded into six T175 flasks. 24 hr later, cells at 60%–70% confluency were transfected with EET construct 5 μg, pAAV-RC 5 μg, p-Helper 5 μg, TurboFect 30 μl, and OptiMEM up to 2 ml (For each T175 flask). Following 48 to 72 hr, the cells were harvested to obtained pellets then resuspended in 10 ml lysis buffer (150 mM NaCl, 50 mM Tris–HCl pH 8.5, 2 mM $MgCl_2$). Then the cell suspension was subjected to four rounds of freeze/thaw by alternating the tubes between the dry ice-ethanol bath and the 37°C water bath, vortexing briefly after each thaw. The lysates were cleared by centrifugation at 10,000x *g* for 10 min and treated with 8 μl of benzonase nuclease (Sigma-Aldrich). The virus was concentrated and purified using AAV Purification ViraKit™, according to the manufacturer instructions (http://www.virapur.com/files/AAV_3Pack_3061,_3063_1j_LR.pdf). 16 μl of the concentrated virus was spared for titer quantification. They were treated with RQ1

DNase (Promega), and then half the amount was heated at 95°C for 10 min to denature the capsids and release the ssDNA of the virus. Then the titer of the virus was determined by qRT-PCR using Fast SYBR ready mix (ABI) with the following primers: qRT-PCR_Puro_FW ACAGATGGAAGGCCTCCTG and qRT-PCR_Puro_Rev CAGACCCTTGCCCTGGTG. Standard curve was prepared using the EET construct. The PCR conditions were as follows: Holding Stage 95°C for 3 min; Cycling stage 95°C for 3 s then 60°C for 30 s (40 cycles).

2.5 | Generation of EET clones

A total of 100,000 cells of interest were seeded into six-well plates. 24 hr later, the cells were infected with 100,000 MOI of the relevant virus, diluted in 0.6 ml optimum. After 6 hr, fresh media were added for additional 72 hr. The cells were harvested and seeded in 96-well plates at a density of 500 cells/well. 24 hr later, puromycin was added. Fresh media were added to the cells including puromycin at least once a week (according to the proliferation rate of the cells). During this period, single colonies were monitored and consolidated into one 96-well plates. In case, pools were grown (usually in all wells of the plates); one plate was randomly chosen for genomic screen using DirectPCR reagent (Viagen) according to the manufacturer instructions. In case of single clones screen, the control primer and a primer located outside the HAs were used. In pool screen, a primer located within the tagging cassette was used instead of the control primer. Potential colonies were further validated at the mRNA levels following expansion and RNA extraction using RNeasy Mini Kit (Qiagen). cDNA was prepared using iScript™ Reverse Transcription Supermix (Bio-Rad). PCR was performed using primers from the tagging cassette and primers located in exons not included in the HAs. Further validation was made by sequencing the PCR product. Following validation in case of pools, subcloning was performed by diluting the cells in 20% FBS to 1 cell/well in 96-well plate to obtain single clones. Once small clones are obtained fresh media with puromycin was added. Then the single clones were consolidated and screened using the control primers. Positive clones were expanded for validation of protein expression.

2.6 | Western blot and immunoprecipitation assays

Cells were gently washed in PBS and then lysed using lysis buffer (1% NP-40, 50 mM Tris–HCl pH 7.5, 150 mM NaCl, complete protease inhibitor tablet, EDTA-free (Roche), 1 μM sodium orthovanadate, 1 mM sodium fluoride, and 0.1% β-mercaptoethanol). Lysed cells were scraped and transferred into a 1.5-ml microcentrifuge tube. Samples were incubated at 4°C for 20 min and then centrifuged for 15 min at 17,000x *g* at 4°C. Proteins (50 μg) were resolved on 10% SDS-polyacrylamide gels and transferred to nitrocellulose membranes (Bio-Rad). Alternatively, the cleared cell lysates were incubated with anti-Flag M2 affinity agarose beads (Sigma-Aldrich), overnight at 4°C. Then the beads were washed three times with the lysis buffer then resuspended with sample buffer and then resolved on 10% SDS-polyacrylamide gels and transferred to nitrocellulose membranes (Bio-Rad). Western blots were probed with the following antibodies: anti-Flag (M2) (Sigma-Aldrich), anti-c-NRAS (F155-277, Millipore), anti-NRAS (sc-519, Santa Cruz), anti-c-CBL (2747, Cell signaling), and anti-αtubulin (Millipore).

2.7 | Estimating the copy number of the *NRAS* alleles

The copy number was determined by qRT-PCR using Fast SYBR ready mix (ABI). For the reaction mix, 3 ng of genomic DNA was used, 1 μl of 10 μM stock solution of each primer, 5 μl of the master mix, and the reaction was adjusted to 10 μl. The PCR conditions were as follows: 95°C 5 min, (95°C 15 s, 58°C 30 s, and 70°C 30 s) × 40 cycles. LINE1 was used as an endogenous control using the following primers: forward- AAAGCCGCTCAACTACATGG and reverse- TGCTTTGAATGCGTCCCAGAG. The sequences of the NRAS primers were as follows: forward- CGCCAGTACCGAATGAAAAAA and reverse- ACACATGGCAATCCCATACAAC. The mean of the cycles of NRAS and the LINE1 of all samples was used as the reference sample to retrieve the value of the relative quantification (RQ). For estimating the genotype of the amplified allele, the region of the Q61R/K mutation was amplified using the forward primer TGTAAAACGACGGCCAGTAACCTCATTTCCCCATAAAGATT and the reverse primer TGCAGTAGAGTTGTCATTTGAGTT. The PCR was treated with exonuclease (Thermo Scientific) and Shrimp alkaline phosphatase (Thermo Scientific) then sequenced using M13 primer that was embedded to the forward primer.

2.8 | 5-aza Treatment and it effect on the expression of the *NRAS* wt and tagged alleles

A total of 100,000 cells/well of parental and tagged A375 cells were seeded in six-well plate; 24 hr later, the cells were treated with 0.5, 1, 2, and 5 mM 5-Aza-2′-deoxycytidine (Sigma-Aldrich) diluted in 1:1 (Acetic Acid:DDW). 5-Aza was added fresh every 24 hr (stock solution of 20 mM was kept in the −80°C). RNA was extracted after 48 hr of treatment. The change in the expression was estimated by semiquantitative PCR of *NRAS* and *PAC* in the *wt* and tagged cells, respectively. Actin was used to normalize the intensity of the bands (the sequence of the primers is described in Table S2).

2.9 | Proteomic analysis of tagged *NRAS* binding partners

A375 single clone of tagged NRAS named A4 was starved for 16 hr and then activated with EGF (100 ng/ml, Sigma-Aldrich) that was added to the media for 15 min then the cells were lysed as described above. Three milligrams of the proteins lysates were taken for immunoprecipitation with anti-Flag M2 affinity agarose beads as described above and then stained on SDS-PAGE with Imperial blue reagent (Thermo Scientific). The proteins in the gel were reduced with 3 mM DTT (60°C for 30 min), modified with 10 mM iodoacetamide

in 100 mM ammonium bicarbonate (in the dark, room temperature for 30 min), and digested in 10% acetonitrile and 10 mM ammonium bicarbonate with either modified trypsin or chymotrypsin (Promega) at a 1:10 enzyme-to-substrate ratio, overnight at 37°C. The resulted peptides were desalted using C18 tips (Homemade stage tips) dried and resuspended in 0.1% formic acid.

The peptides were resolved by reverse-phase chromatography on 0.075 × 180-mm fused silica capillaries (J&W) packed with Reprosil reversed phase material (Dr Maisch GmbH, Germany). The peptides were eluted with linear 60 min gradient of 5 to 28% 15 min gradient of 28% to 95% and 15 min at 95% acetonitrile with 0.1% formic acid in water at flow rates of 0.15 µl/min. Mass spectrometry was performed by Q Exactive plus mass spectrometer (Thermo) in a positive mode using repetitively full MS scan followed by collision induces dissociation (HCD) of the 10 most dominant ions selected from the first MS scan.

The mass spectrometry data were analyzed using Proteome Discoverer 1.4 software with Sequest (Thermo) and Mascot (Matrix Science) algorithms against human UniProt database with mass tolerance of 10 ppm for the precursor masses and 0.05 amu for the fragment ions. Oxidation on Met was accepted as variable modifications, and carbamidomethyl on Cys was accepted as static modifications. Minimal peptide length was set to six amino acids, and a maximum of two miscleavages was allowed. Peptide- and protein-level false discovery rates (FDRs) were filtered to 1% using the target-decoy strategy. Protein table was filtered to eliminate the identifications from the reverse database and from common contaminants. Semiquantitation was performed by calculating the peak area of each peptide based its extracted ion currents (XICs), and the area of the protein is the average of the three most intense peptides from each protein.

2.10 | Inhibition of farnesyltransferase in NRAS tagged melanoma cells

The farnesyl transferase inhibitor lonafarnib (Sigma-Aldrich) was used. The inhibitor was dissolved in DMSO and was added directly to the culture medium of melanoma cells at different concentrations for 24 hr. Melanoma cells were incubated with culture medium or culture medium with DMSO as controls. Cells were lysed as described above, and 3 mg were immunoprecipitaed with anti-Flag M2 affinity agarose beads followed by Western blot with anti-NRAS antibody (sc-519, Santa Cruz).

2.11 | Construction of expression vectors for wt and mutant NRAS

Human NRAS cDNA (NM_002524) was cloned from HEK293T cDNA using PfuUltra II HotStart PCR Master Mix (Agilent Technologies) according to the manufacturer's instructions and the forward and reverse primers listed in Table S2. A sequence encoding a Flag tag at the N' terminus of NRAS was introduced during the cloning procedure. PCR products were cloned into the pCDF1-MCS2-EF1-Puro vector (Systems Biosciences) via the XbaI and NotI restriction sites. The mutation encoding Q61R was introduced using fusion PCR site-directed mutagenesis. The NRAS constructs were transiently transfected into A375 melanoma cells using Lipofectamine 2000 (Life Technologies) as described by the manufacturer. Cells were incubated for 48 hr after transfection before protein extraction and immunoprecipitation with Flag beads as described above.

ACKNOWLEDGEMENT

Y.S. is supported by the Israel Science Foundation grant number 696/17. This project has received funding from the European Research Council (ERC) under the European Union's Horizon 2020 research and innovation program (grant agreement No 754282), the ERC (StG-335377), the MRA, the Henry Chanoch Krenter Institute for Biomedical Imaging and Genomics, the Estate of Alice Schwarz-Gardos, the Estate of John Hunter, the Knell Family, the Peter and Patricia Gruber Award, and the Hamburger Family. M.K. is supported by an Israel Science Foundation grant number 1454/13.

ORCID

Yardena Samuels http://orcid.org/0000-0002-3349-7266

REFERENCES

Bitinaite, J., Rubino, M., Varma, K. H., Schildkraut, I., Vaisvila, R., & Vaiskunaite, R. (2007). USER™ friendly DNA engineering and cloning method by uracil excision. *Nucleic acids research*, *35*, 1992–2002. https://doi.org/10.1093/nar/gkm041

Burd, C. E., Liu, W., Huynh, M. V., Waqas, M. A., Gillahan, J. E., Clark, K. S., … Souroullas, G. P. (2014). Mutation-specific RAS oncogenicity explains NRAS codon 61 selection in melanoma. *Cancer discovery*, *4*, 1418–1429. https://doi.org/10.1158/2159-8290.CD-14-0729

Chevalier-Mariette, C., Henry, I., Montfort, L., Capgras, S., Forlani, S., Muschler, J., & Nicolas, J.-F. (2003). CpG content affects gene silencing in mice: Evidence from novel transgenes. *Genome biology*, *4*, R53. https://doi.org/10.1186/gb-2003-4-9-r53

Chuang, E., Barnard, D., Hettich, L., Zhang, X.-F., Avruch, J., & Marshall, M. S. (1994). Critical binding and regulatory interactions between Ras and Raf occur through a small, stable N-terminal domain of Raf and specific Ras effector residues. *Molecular and cellular biology*, *14*, 5318–5325. https://doi.org/10.1128/MCB.14.8.5318

Erijman, A., & Shifman, J. M. (2016). RAS/Effector interactions from structural and biophysical perspective. *Mini reviews in medicinal chemistry*, *16*, 370–375. https://doi.org/10.2174/1389557515666151001141838

Hunter, J. C., Manandhar, A., Carrasco, M. A., Gurbani, D., Gondi, S., & Westover, K. D. (2015). Biochemical and structural analysis of common cancer-associated KRAS mutations. *Molecular cancer research*, *13*, 1325–1335. https://doi.org/10.1158/1541-7786.MCR-15-0203

Kho, Y., Kim, S. C., Jiang, C., Barma, D., Kwon, S. W., Cheng, J., … Falck, J. (2004). A tagging-via-substrate technology for detection and proteomics of farnesylated proteins. *Proceedings of the National Academy of Sciences of the United States of America*, *101*, 12479–12484. https://doi.org/10.1073/pnas.0403413101

Kim, J.-S., Bonifant, C., Bunz, F., Lane, W. S., & Waldman, T. (2008). Epitope tagging of endogenous genes in diverse human cell lines. *Nucleic acids research*, *36*, e127–e127. https://doi.org/10.1093/nar/gkn566

Loh, M. L., Sakai, D. S., Flotho, C., Kang, M., Fliegauf, M., Archambeault, S., … Bueso-Ramos, C. E. (2009). Mutations in CBL occur frequently in juvenile myelomonocytic leukemia. *Blood*, *114*, 1859–1863. https://doi.org/10.1182/blood-2009-01-198416

Mutskov, V., & Felsenfeld, G. (2004). Silencing of transgene transcription precedes methylation of promoter DNA and histone H3 lysine 9. *The EMBO Journal*, *23*, 138–149. https://doi.org/10.1038/sj.emboj.7600013

Network, C. G. A. (2015). Genomic classification of cutaneous melanoma. *Cell*, *161*, 1681–1696.

Nihal, M., & Wood, G. S. (2016). c-CBL regulates melanoma proliferation, migration, invasion and the FAK-SRC-GRB2 nexus. *Oncotarget*, *7*, 53869.

Nussinov, R., Tsai, C.-J., Chakrabarti, M., & Jang, H. (2016). A new view of Ras isoforms in cancers. *Cancer research*, *76*, 18–23. https://doi.org/10.1158/0008-5472.CAN-15-1536

Porteus, M. H., Cathomen, T., Weitzman, M. D., & Baltimore, D. (2003). Efficient gene targeting mediated by adeno-associated virus and DNA double-strand breaks. *Molecular and cellular biology*, *23*, 3558–3565. https://doi.org/10.1128/MCB.23.10.3558-3565.2003

Schmidt, M. H., & Dikic, I. (2005). The Cbl interactome and its functions. *Nature reviews Molecular cell biology*, *6*, 907–919. https://doi.org/10.1038/nrm1762

Schnepp, B. C., Jensen, R. L., Chen, C.-L., Johnson, P. R., & Clark, K. R. (2005). Characterization of adeno-associated virus genomes isolated from human tissues. *Journal of virology*, *79*, 14793–14803. https://doi.org/10.1128/JVI.79.23.14793-14803.2005

Stephen, A. G., Esposito, D., Bagni, R. K., & Mccormick, F. (2014). Dragging ras back in the ring. *Cancer Cell*, *25*, 272–281. https://doi.org/10.1016/j.ccr.2014.02.017

Zhang, X., Guo, C., Chen, Y., Shulha, H. P., Schnetz, M. P., Laframboise, T., … Scacheri, P. C. (2008). Epitope tagging of endogenous proteins for genome-wide ChIP-chip studies. *Nature methods*, *5*, 163–165. https://doi.org/10.1038/nmeth1170

SUPPORTING INFORMATION

Additional supporting information may be found online in the Supporting Information section at the end of the article.

How to cite this article: Alon M, Emmanuel R, Qutob N, et al. Refinement of the endogenous epitope tagging technology allows the identification of a novel NRAS binding partner in melanoma. *Pigment Cell Melanoma Res*. 2018;31:641–648. https://doi.org/10.1111/pcmr.12705

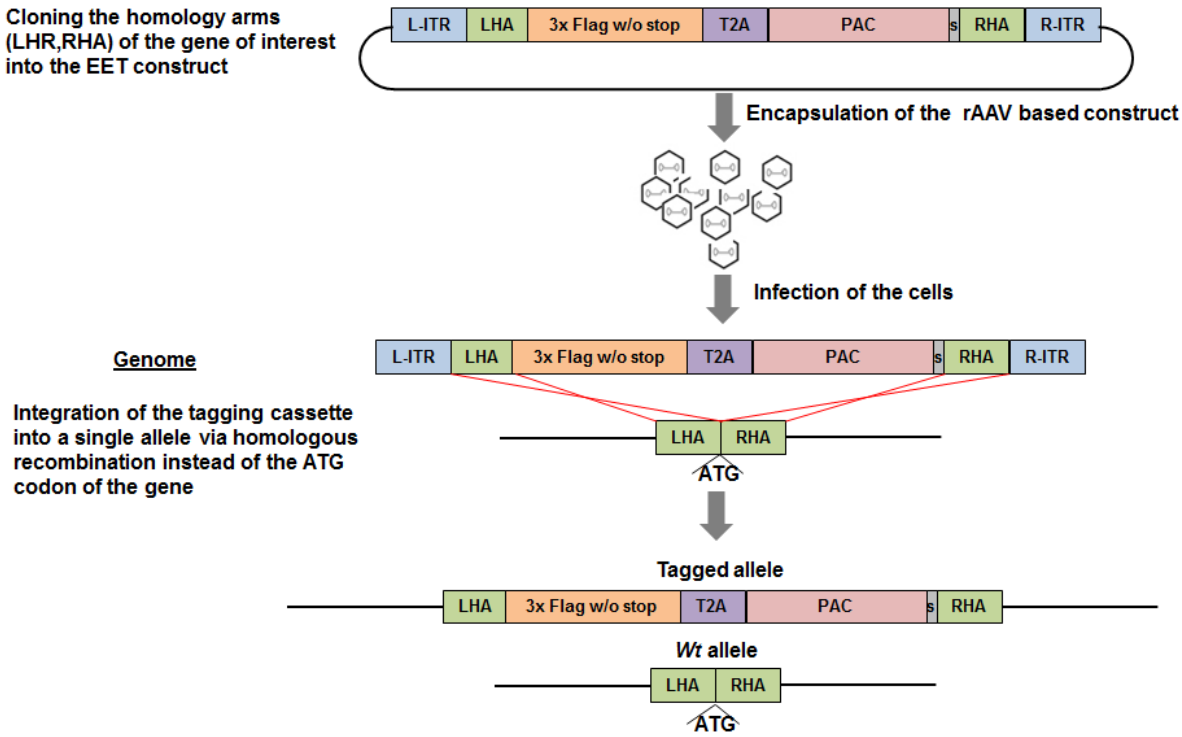

Supplementary Figure 1. A schematic description of the EET approach at the N-terminus. Genomic sequences of ~1Kbps flanking the ATG codon of the gene of interest are amplified and cloned into a tagging construct comprises of an epitope and a selection marker in a rAAV backbone. The region located upstream to the ATG codon designated left homology arm (LHA) and the region downstream is designated right homology arm (RHA). The sequences from the left to the right inverted terminal repeats (L-ITR and R-ITR, respectively) are encapsulated as ssDNA rAAV particles. The virus particles are then added onto cells and following infection the ssDNA can be integrated into the genome through homologous recombination (HR) process (red lines) via the homology arms located in the virus particles and the genomic sequence of the gene. Since HR is considered a rare event, only on allele is tagged. (T2A - thosea asigna virus 2A self-cleaving peptide, PAC- Puromycin N-acetyltransferase, S – sheGFP recognition site).

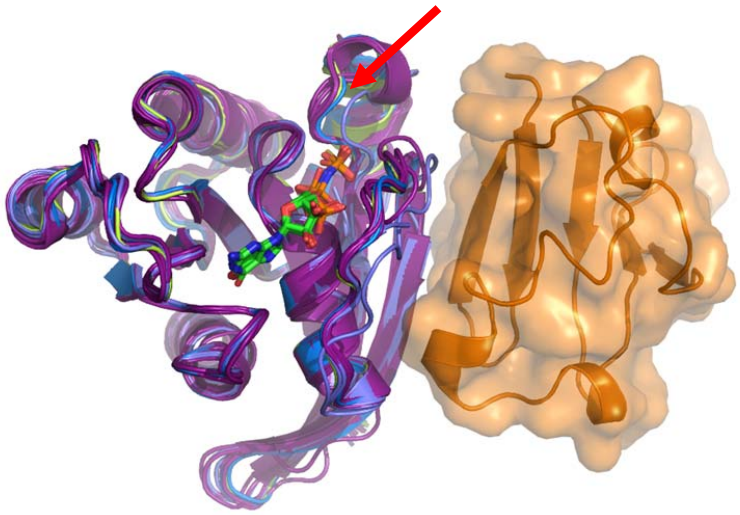

Supplementary Figure 2: Wt Ras and Q61 Ras mutants adopt very similar 3D conformations and are expected to bind effectors similarly. The following 16 crystal structures of activated Ras (with PDB IDs) with bound GTP or GTP analogs were superimposed: wt N-Ras, green (5UHV); wt H-Ras, blue (5P21, 1QRA, 1CTQ); wt K-Ras, cyan (5VQ2, 5VQ6); H-Ras and K-Ras Q61 mutants (H-Ras Q61L, Q61I, Q61K, Q61V and K-Ras Q61L, Q61H), purple (721P, 2RGA, 2RGB, 2RGC, 2RGD, 4G3X, 621P). Ras proteins are shown as ribbons, colored as above. The bound nucleotides are shown as sticks and colored by element. The complex of H-Ras with the Raf-RBD (Ras binding domain) was superimposed using the Ras coordinates, with the Raf-RBD shown as orange ribbon with a transparent molecular surface, for reference. The location of the Q61 residue is marked with a red arrow. The structures of the Ras proteins were extremely similar, with RMSD (Root Mean Square Distance) values for their superimposed backbone atoms smaller than 1Å in all cases, and in most cases, smaller than 0.5Å.

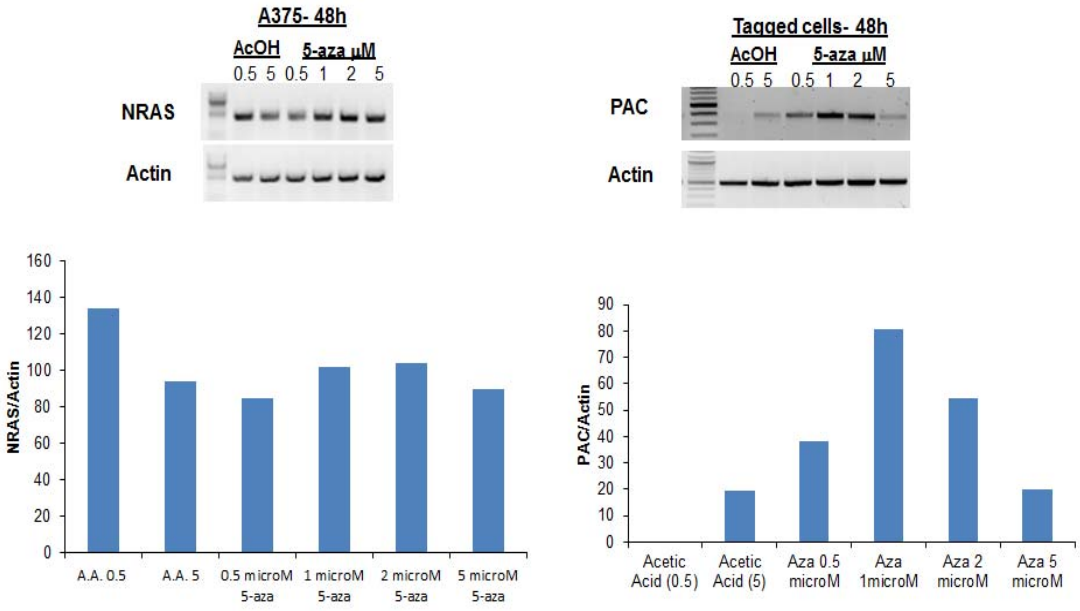

Supplementary Figure 3. Effect of 5-aza on the expression of NRAS and Flag-tagged NRAS in A375 cells. Parental and tagged A375 cells were treated with different concentrations of 5-aza diluted in 50% Acetic Acid (AcOH) of which equivalent dilutions were used as negative control. 48h later RNA was extracted and semi-quantitative PCR was performed using NRAS and PAC primers to measure expression of the parental and tagged NRAS, respectively. Representative gels are described in the upper panel and the graphs represent the mean quantification of the NRAS and PAC bands after normalization with Actin of two independent experiments.

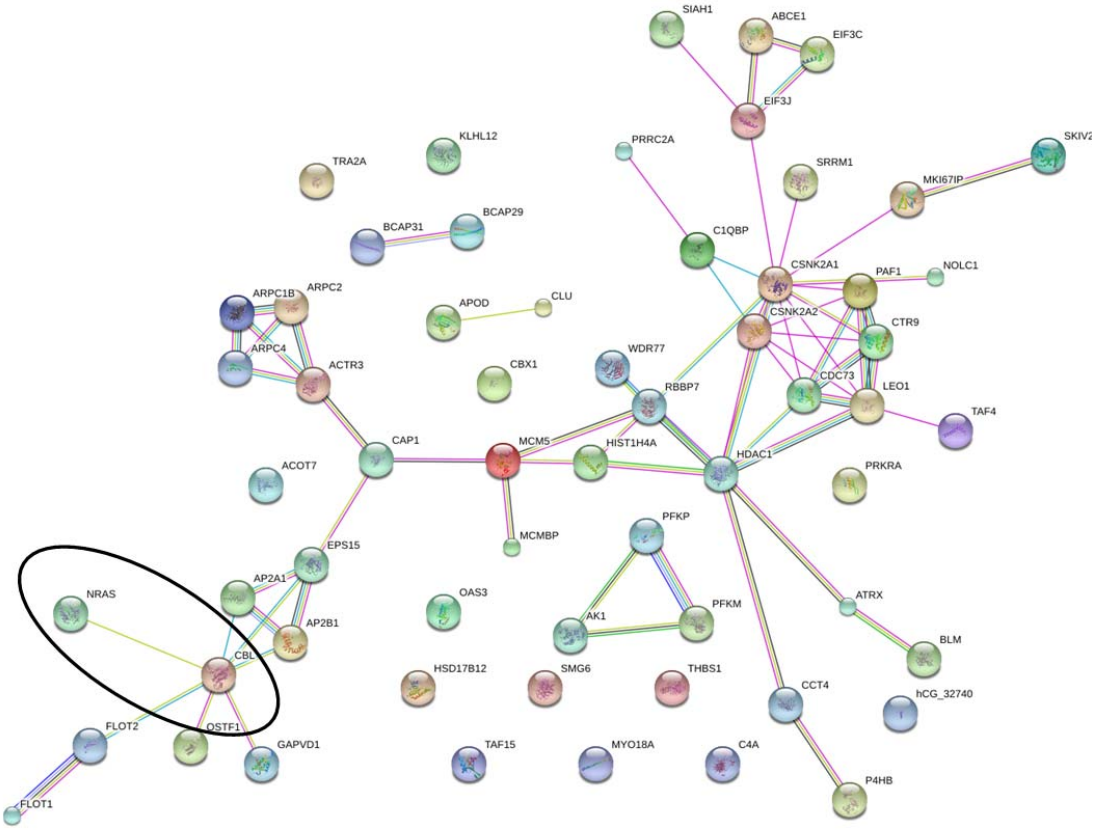

Legend:

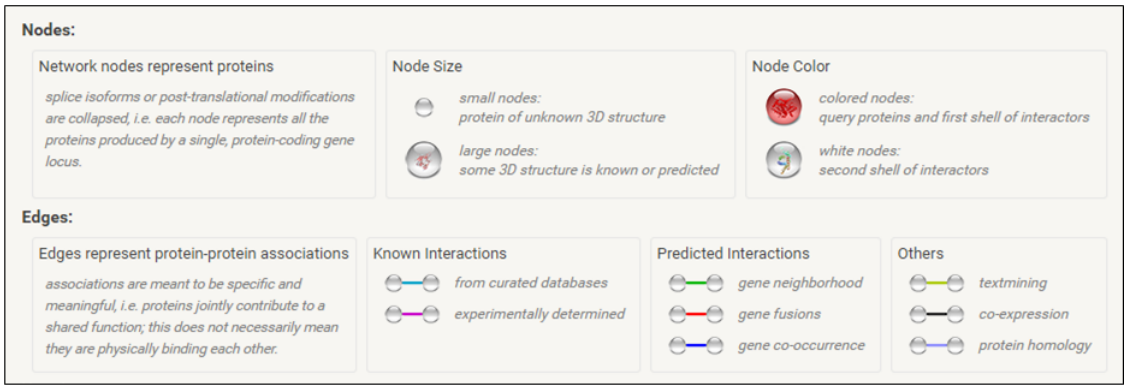

Supplementary Figure 4. String analysis of Flag-NRAS binding partners. String web site (http://string-db.org) was used for analyzing the Flag NRAS protein networks. All of the significant bidning proteins that were identified by mass spec analysis were analyzed by String software to summarize the network of the predicted associations between the proteins. The network nodes are proteins. The edges represent the predicted functional associations. The edge colored lines represent the existence of the seven types of evidence used in

predicting the associations: red line - indicates the presence of fusion evidence, green line - neighborhood evidence, blue line – co-occurrence evidence, purple line - experimental evidence, yellow line – text mining evidence, light blue line - database evidence, black line – co-expression evidence.

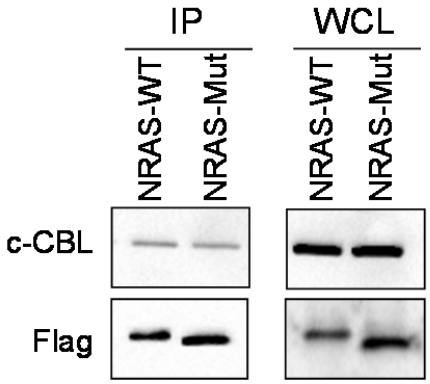

Supplementary Figure 5. NRAS-Q61R binds c-CBL similarly to wt NRAS. Immunoblots of A375 over-expressing wt NRAS or mutant NRAS (Q61R) after immunoprecipitation with anti-Flag beads. Immunoprecipitates were analyzed in parallel by anti-Flag and anti-c-CBL immunoblotting. Flag-NRAS was co-immunoprecipitated with endogenous c-CBL from both wt NRAS and mutant NRAS lysates using anti c-CBL antibody. WCL– whole cells lysate.

Supplamentry Table 1. Efficient N-terminus tagging of *NRAS* in low passage melanoma cells. The table describes the allele copy number of *NRAS* in the cells, the infection efficiency, the multiplicity of infection (MOI), the number of colonies screened and the number of positive colonies. (*pools, #single colony).

Cell	NRAS Genotype	NRAS alleles copy number	% of Infection	MOI	# of colonies screened (genome)	# of positive colonies	of positive clones
A375	WT	2n	~100	$1.2X10^4$	70	28*	**40**
T106	WT	2n	~100	$1.2X10^4$	80	17*	**21**
12T	Q61R	4n	~15	10^5	44	10#	**22**
T17	Q61R	2n	<1	10^5	96	13*	**13**
T110	Q61R	2n	<1	10^5	96	17#	**18**

Supplementary Table 2 – Primers list

Primer Name	Primer Sequence (5'-3')
Primers used for the construction of pT2A-Puror-User-C'	
1. Cloning of the HA-tag	
SpeI_linker_HA_FW	TCAGCactagtATCTCATCCTCCGGGGCACTTGATTATGATATTCCAACTACTGCTAGCGAGAATTTGTATTTTC
EcoRI_linker_HA_Rev	ctgccgaattcAGCGTAATCTGGAACATCGTATGGGTAGAGCTCACCCTGAAAATACAAATTCTCGCTAGCAGTAG
2.Cloning of T2A	
EcoRI_T2A_FW	cccccgaattcggcagtggtGAGGGCAGAGGAAGTCTGCTAACATGCGGTGACGTCG
MluI+BglII_T2A_Rev	cccccACGCGTagatctgcTGGGCCAGGATTCTCCTCGACGTCACCGCATGTTAGC
3. Cloning of PAC_without ATG+shEGFP	
BglII_PAC_FW	CCAgcagatctCccgagtacaagcccacggt
EcoRV+NdeI+T3+sheGFP_PAC_Rev	TCAGCgatatccctaggccgcggCTTTAGTGAGGGTTAATTGCGCCATATGatagacgttgtggctgttgtatcaggcaccgggcttgcgggt
Primers used for the construction of pT2A-Puror-User-N'	
1. Eliminating an ATG in the LHA cloning cassette	
AgeI_LHA cloning cassette_FW	CCGGTGCTGAGGGAAAGTCTAGAGGATCCTCTAGACGTCTCCTCAGCACTAGTGCCAC
SpeI_LHA cloning cassette_Rev	CATGGTGGCACTAGTGCTGAGGAGACGTCTAGAGGATCCTCTAGACTTTCCCTCAGCA
2. Cloning of PAC+shEGFP	
SpeI_PAC_FW	TCAGCACTAGTGCCACCATGGCCACCGAGTACAAGCCCACGGT
EcoRI_PAC+sheGFP_Rev	CTGCCGAATTCGATATAGACGTTGTGGCTGTTGTAGTTGGCACCGGGCTTGCGGGT
3.Cloning of 3xFlag-tag	
BglII_3xFlag_FW	CCCAGCAGATCTCGACTACAAAGACCATGACGGTGATTATAAAGATCATGACATCGACTACAAGG
EcoRV_3xFlag__Rev	TCAGCGATATCCTTGTCATCGTCATCCTTGTAGTCGATGTCATGATC
Primers used for the cloning of the HA	
N'NRAS_ LHA_FW	gggaaaguCCAGTTTTCTGTTAATGGCGAAAGA
N'NRAS_ LHA+Analysis_Rev	ggagacguggtaaagatgatccgacaagtgaTTCACACCAGCAAGAACctgttg
N'NRAS_RHA_FW	ggtcccauggACTGAGTACAAACTGGTGGTGGTTG
N'NRAS_ RHA_Rev	ggcataguGAGCCTTAGGTGCCACTTACTGAAGA
Primers used for the genomic screen	

PAC_LHA_analysis_Rev	GTGGGCTTGTACTCGGTCAT
T3_RHA_FW	GCGCAATTAACCCTCACTAAAG
NRAS_LHA_analysis_FW	CGGTTTTATCTTCCCCCTTG
PAC_LHA_analysis_Rev	GTGGGCTTGTACTCGGTCAT
NRAS_LHA_analysis_Rev	GGTAAAGATGATCCGACAAGTGA
Primers used for cDNA validation	
EET_C'_LHA_screen_Rev1	cAGCGTAATCTGGAACATCG
EET_C'_LHA_screen_Rev2	CAGACTTCCTCTGCCCTCac
PAC_cDNA_FW	caccagggcaagggtctg
NRAS_exon4&5_Rev	AACACCCTGTCTGGTCTTGG
NRAS_seq_Rev (used for sequencing the PCR products)	TCGCTTAATCTGCTCCCTGT
Oligose used for the cloning of the sheGFP into pLKO1-neo	
sheGFP_FW	CCGGTACAACAGCCACAACGTCTATCTCGAGATAGACGTTGTGGCTGTTGTATTTTTG
sheGFP_Rev	AATTCAAAAATACAACAGCCACAACGTCTATCTCGAGATAGACGTTGTGGCTGTTGTA * Sequence in red represents the hairpin
Primers used for NRAS cloning in expression vectors	
NRAS_F	ACTGAGTACAAACTGGTGGT
NRAS_R	TTACATCACCACACATGGCA